ARTICLES

Optical properties and electronic structures of Ni_3Al alloys

Joo Yull Rhee
Department of Physics, College of Natural Sciences, Hoseo University, Asan, 336-795 Choongnam, Korea

B. N. Harmon and D. W. Lynch
Ames Laboratory-U.S. Department of Energy and Department of Physics and Astronomy, Iowa State University, Ames, Iowa 50011
(Received 10 July 1995; revised manuscript received 2 August 1996)

The dielectric functions of Ni_3Al polycrystalline alloys were measured by spectroscopic ellipsometry in the energy range of 1.5–5.4 eV. The samples were $Ni_{1-x}Al_x$ alloys with $x=0.2625,0.2525,0.25,0.244$, and 0.2359. One broad peak was observed in the optical-conductivity spectra around 4.4 eV. The band structures and the optical conductivity were calculated in the Au_3Cu structure with the linearized-augmented-plane-wave method. By including both energy-dependent broadening and an approximate self-energy correction the calculated optical-conductivity spectrum gives quite good agreement with experiment. The calculation shows that the main contribution to the 4.4 eV peak comes from the **k** points close to the Γ-M-R plane and near the midpoints of the X-M line and Γ-M line. [S0163-1829(97)03008-7]

$Ni_{1-x}Al_x$ intermetallic compounds have received considerable attention because of their unusual physical properties. It forms very stable $B2$ phase (cubic CsCl structure) with $0.4 \leqslant x \leqslant 0.55$ and undergoes martensitic transformation from $B2$ phase to face-centered-tetragonal phase for x near 0.38.[1] The Ni_3Al compounds exhibit weak itinerant ferromagnetism with $T_c=41$ K and strong exchange-enhanced paramagnetic properties for 73.5–74.5 at. % Ni concentrations.[2] Dhar *et al.*[3,4] measured the heat capacity of Ni_3Al alloys under the influence of magnetic fields in the 1.5–20 K range and found an upturn in C/T-versus-T^2 plots in the low temperature region. They interpreted the upturn as an indication of the enhancement of the effective electronic mass due to spin fluctuations.

The energy band structures of Ni_3Al were calculated several times to understand the magnetic properties of the alloys.[5,6,8–10] Hackenbracht and Kübler[5] calculated the paramagnetic band structures of Ni_3Al, NiAl, and $NiAl_3$ and the spin-polarized band structure for Ni_3Al using the augmented-spherical-wave (ASW) method. Using the local-density approximation for the paramagnetic calculations and the local spin density approximation for the spin-polarized calculation, they calculated various physical quantities such as the density of states, the magnetic moment and its pressure derivative, lattice constants, bulk modulus, and heats of formation. Their calculated magnetic moment of Ni_3Al is $m=0.092\mu_B$ per unit cell, which is only 40% of the experimental value.[11] Later Buiting, Kübler, and Mueller[6] used the same method to derive a high-precision density of states of Ni_3Al. By comparing the calculated specific heat with the experiment they concluded that Ni_3Al was still in the fluctuation regime even though it is in a ferromagnetic state. They found that the magnetic moment almost vanishes at the experimental lattice constant (3.568 Å=6.743 a.u.) while it is $0.203\mu_B$ per unit cell, which is close to the experimental value of $0.23\mu_B$ per unit cell,[11] at a lattice constant of 3.583 Å(=6.771 a.u.).

Min, Freeman, and Jansen[8] used the self-consistent full-potential linearized-augmented-plane-wave (LAPW) method to investigate the electronic structure and magnetic properties of Ni_3Al. They performed both paramagnetic and spin-polarized calculations. The energy of the ferromagnetic state is slightly ($\sim$1 mRy) lower than the paramagnetic state at the experimental lattice constant. The calculated magnetic moment was $0.15\mu_B$ per Ni atom and the total moment was $0.44\mu_B$ per cell. Although the calculated total moment was twice as large as observed, the authors argued that the spin-orbit interaction might reduce the calculated magnetic moment to $0.26\mu_B$ per cell, since the spin-orbit interaction reduced the exchange splitting by $\sim$40%. Xu *et al.*[9] studied the structural stability of Ni_3Al using an all-electron self-consistent local-density linear-muffin-tin-orbital (LMTO) method for different crystal structures and for different phases; cubic ($L1_2$), tetragonal ($D0_{22}$), and hexagonal ($D0_{19}$). They found that the (weakly) ferromagnetic cubic structure is the most stable phase. Their calculated magnetic moment ($0.71\mu_B$ per cell) was even larger than that of Ref. 8, however, they found that it was reduced remarkably to $0.46\mu_B$ per cell if the spin-orbit interaction was included. In this paper we are concerned with room temperature optical experiments and our calculations are therefore for the paramagnetic state. Since two states, one above the Fermi level and one below the Fermi level, are involved in the optical transitions, the measurements in optical properties can give us more information about the electronic structures of the alloys.

Khan *et al.*[10] used the self-consistent LMTO method within the atomic sphere approximation to calculate the band structure and the optical conductivity. They calculated the

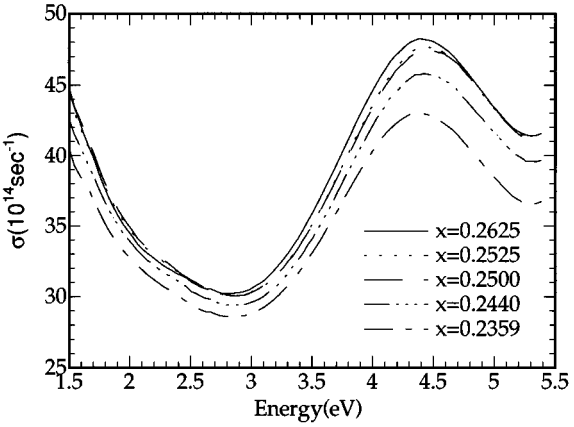

FIG. 1. Optical conductivities of $Ni_{1-x}Al_x$ alloys. Note that the zero of the optical conductivity is suppressed.

optical-conductivity spectra with and without the inclusion of the dipole-transition-matrix elements and found that the inclusion of the matrix elements is very crucial to make the calculated spectra coincide with the measured one. They also suggested that broadening and self-energy corrections may improve the agreement between the experiment and the theory.

The dielectric function of Ni_3Al was measured by spectroscopic ellipsometry in the 0.5–5.3 eV region by van der Heide *et al.*[12] The optical-conductivity spectrum showed a weak shoulder at 0.86 eV and a broad, pronounced peak at 4.32 eV. The authors claimed that the experimental results are in good agreement with the theory in which they calculated the spectrum using the band structure of Ref. 6 without inclusion of the dipole-transition-matrix elements.

In this work we report experimental and theoretical results of the optical-conductivity spectra of Ni_3Al alloys. The measured optical conductivity is almost 50% larger than that of Ref. 12 in the 1.5–5.4 eV range. In the course of the optical-conductivity calculation we included the dipole-transition-matrix elements. After the theoretical optical-conductivity spectrum was obtained an energy-dependent broadening was applied. The broadened spectrum was further fitted to the experimental one using λ-fitting procedure (see text below). The λ fitting, which is originated from a simplified attempt to account for the self-energy correction to the excited states,[7] is particularly important because it markedly improves the agreement between the experimentally and theoretically determined peak positions. The calculated optical-conductivity spectrum before broadening and after applying the λ fitting is very similar to that of Ref. 10, however, our interpretation differs.

The samples were those of Refs. 3 and 4. They were mechanically polished with a series of alumina powders down to 0.05 μm diameter. The samples were then cleaned using acetone and methanol in an ultrasonic cleaner. We measured the dielectric functions using a spectroscopic rotating-analyzer ellipsometer[13] at room temperature. We did not put the sample in the vacuum chamber. Therefore the sample surface was covered by an oxide film whose maximum thickness $\sim$50 Å might cause errors in measurement up to about 1%.[12]

The measured optical-conductivity spectra are shown in Fig. 1. The overall shape of spectrum and the position of the broad peak at 4.4 eV are in good agreement with the previous measurement of Ref. 12. However, there is a large difference in the magnitude of the optical conductivity. Our measurement is almost 50% larger than that of Ref. 12. The difference is probably due to the surface roughness of the sample. In Ref. 12 the authors used 1 μm diam diamond powder, which is significantly larger than our final grade of alumina powder (0.05 μm). The large diameter of the polishing powder makes the sample surface rougher and the surface roughness of the sample is approximately the same order of the final grade of the polishing powder. In addition, diamond powder is harder and therefore can severely damage the sample surface more than alumina. The rougher the sample surface the smaller the reflectivity and, in turn, the smaller the optical conductivity. To check this point we applied the three-phase model to simulate the spectrum of Ref. 12 in which the rough overlayer was modeled as a mixture of void and bulk material with a void fraction f_v and thickness d. We used the Bruggeman effective medium approximation[14] to obtain the dielectric function of the overlayer. For the dielectric function of the bulk we used our experimental data. If f_v is small the dielectric function of the overlayer is given by[15]

$$\tilde{\epsilon}_o \simeq \tilde{\epsilon}\left(1-3f_v\frac{\tilde{\epsilon}-1}{2\tilde{\epsilon}-1}\right), \tag{1}$$

where $\tilde{\epsilon}_o$ and $\tilde{\epsilon}$ are the dielectric functions of the overlayer and the bulk, respectively. $f_v=0.14$ and $d=$ 926 Å give a spectrum very close to that of Ref. 12. Although they measured the dielectric functions in an UHV chamber, the effect of a rough surface, about 900 Å thick, is larger than that of the oxide overlayer 50 Å thick.[12]

We also observed the broad and pronounced peak at 4.4 eV but could not observe the weak shoulder at 0.86 eV because it is outside the spectral limit of our measurement system.

To determine the origin of the 4.4 eV peak we performed band structure and optical-conductivity calculations for the paramagnetic phase using the LAPW method[16] in the local-density approximation.[17] The lattice constant was 3.568 Å (=6.7425 a.u.) and the muffin-tin radii were 1.231 Å (=2.3265 a.u.) and 1.270 Å(=2.400 a.u.) for Al and Ni, respectively. A muffin-tin potential was used. The calculated energy band structure along high-symmetry lines is shown in Fig. 2. The band structure and the density of states are similar to those obtained in previous calculations.[5,6,8,9] The only notable difference in the band structures between ours and that of Ref. 12 and Ref. 8 is the energy location of the 16th band at the R point and the shape of this band along the M-R-X direction. In Ref. 8 it is located only 0.1 eV below the Fermi level E_F, and has a local maximum at the R point, while in Ref. 12 and our work it is located 0.5 eV below E_F and has a local minimum at the R point along the M-R-X direction, but has a local maximum near the R point along the R-X direction.

The band structure of Ref. 10 is different from ours and that of Ref. 12 at a few points. First, there are missing bands such as the 13th band in the Γ point and the 16th bands at the X, M, and R points if they are compared to our and the

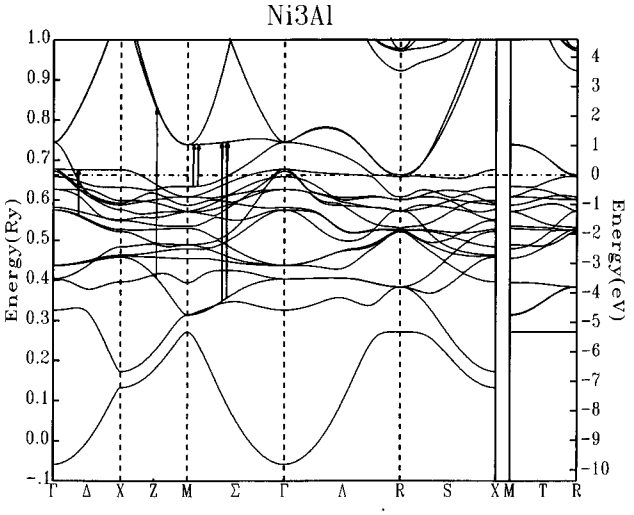

FIG. 2. Band structure of Ni_3Al in the Au_3Cu structure along high-symmetry lines. The optical direct interband transitions corresponding to the 1 eV and 4.4 eV peaks are denoted by the short arrows and long arrows, respectively.

other band structures.[8,12] Second, the splitting between the 16th and 17th bands at one third of Γ-X direction is rather large, while our calculation shows almost no splitting. In Ref. 10 it is not clear that the calculation includes spin-orbit coupling, while we included the spin-orbit coupling during the self-consistent calculation. This may explain why the 17th, 18th, and 19th band at the R point do not split in Ref. 10 while they do in our calculation. In Ref. 12 and Ref. 8 (no spin-orbit coupling) these bands are not split and are occupied. In our calculation the 17th band is split from the 18th and the 19th bands and the 17th band is occupied. Third, the 17th band is unoccupied all along the R-X direction in Ref. 10, however, a fairly large portion of the 17th band in the R-X direction is occupied for our case and others.[8,12]

In Ref. 12 the authors compared the experimental spectrum to the theoretical one by using the band structure calculation of Ref. 6, and they did not include the dipole-transition matrix elements, in other words, they evaluated just the joint density of states divided by the angular frequency of the incident photon (J_{DOS}/ω). The calculated J_{DOS}/ω spectrum shows two peaks (at 3.4 eV and 3.9 eV) close to the experimental peak at 4.4 eV and the authors assigned these peaks as the origin of the experimental one even though their energies are smaller than the experimental one. They also identified the peaks as transitions from bands 3, 4, 5, and 6 to bands 14, 15, and 16 in the neighborhood of the Γ point. However, the inclusion of the dipole-transition matrix elements is essential for optical-conductivity calculations and frequently gives completely different results from a J_{DOS}/ω analysis. Indeed our results and those of Ref. 10, which included the dipole-transition matrix elements in the optical-conductivity calculation, show significantly different spectra and thus our interpretation is different from that given in Ref. 12.

As we see in Fig. 3, the shape of the calculated optical-conductivity spectrum with the dipole-transition matrix elements is very similar to that of Ref. 10. However, there is a discrepancy in the magnitudes. In Ref. 10 the calculated

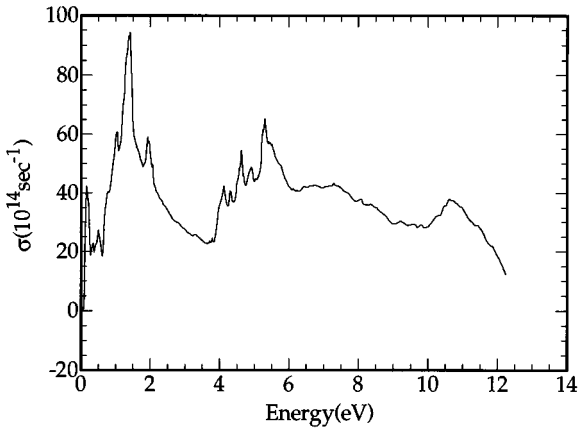

FIG. 3. Theoretical optical conductivity of Ni_3Al before broadening.

spectrum (see Fig. 4 of Ref. 10) shows that the magnitude of the 6.0 eV peak is $\sim 2.9\times 10^{15}$ sec^{-1}, which is close to the magnitude of the 4.32 eV peak of Ref. 12 ($\sim 3\times 10^{15}$ sec^{-1}), while it is only $\frac{2}{3}$ of our measurement. Since the calculated spectrum shows sharp structures, which are not present in a real experiment because of lifetime effects and the experimental spectral resolution, it should be broadened if theory is to have any chance to agree with experiment. Broadening reduces the magnitude of peaks and smears out many sharp structures. The calculated spectrum can be ''adjusted'' to the measured one in the peak position by a λ-fitting procedure (see Fig. 2), however, it is very hard to match the magnitude if the theoretical result of Ref. 10 is used. Meanwhile our calculation is almost twice as large in magnitude as that of Ref. 10. Our calculation also shows some sharp peaks below 1 eV and broad peaks around 7.5 eV and 11 eV. These are missed or too weak to be discernible in the calculation of Ref. 10.

The calculated optical conductivity was broadened using an energy-dependent Lorentzian broadening function of width $\Gamma(E)=AE^2/\mathrm{eV}$, where $E=[E_f(\mathbf{k})-E_i(\mathbf{k})]$ in eV, to simulate the imaginary part of the quasiparticle self-energy. We set the upper limit of $\Gamma(E)_{\max}=2$ eV for agreement be-

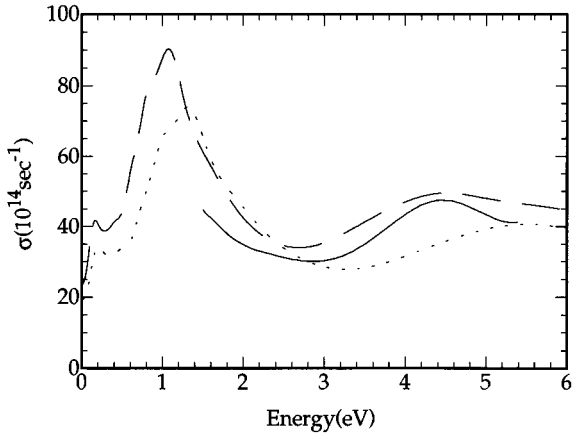

FIG. 4. Experimental (solid line) and theoretical optical conductivities of Ni_3Al. The theoretical ones are calculated with (dashed line) and without (dotted line) the λ fitting after broadening.

tween experiment and calculation. The broadened, calculated spectrum shows a broad peak around 5.5 eV which is higher in energy than the experimental one. To account for this discrepancy we used a λ fitting which has the effect of changing the excited-state energies $\hat{E}_n(\mathbf{k})$ relative to the energies $E_n(\mathbf{k})$ calculated from the ground-state potential, given by[7]

$$\hat{E}_n(\mathbf{k}) = E_n(\mathbf{k}) + \lambda[E_n(\mathbf{k}) - E_F]. \tag{2}$$

Although the parameter λ is dependent on the band index n and the wave vector $\mathbf{k}$, we assumed it constant. Thus a positive λ has the effect of raising the energies of states above and lowering those below E_F; and hence the peaks in the ''bare'' excitation spectrum are shifted to higher energy. A negative λ shifts bare peaks to lower energies. While we have written Eq. (2) as a self-energy correction to individual states (following Ref. 7), this is perhaps misleading, in that we are using a rather simplified correction which is being imposed for the purpose of fitting the excitation spectrum. It is really only concerned with the difference of the self-energy corrections (for the initial and final states). Thus a negative λ is likely to arise from a large positive self-energy correction on the initial state and a small (positive) correction to the final state. This is indeed a highly simplified procedure to avoid the very complicated task of evaluating individual state self-energy corrections.

We can now calculate the corrected optical constants, however, three different forms of equations are given in the literature. In Ref. 7 the imaginary part of the dielectric function is

$$\hat{\epsilon}_2(\omega) = \frac{1}{1+\lambda}\epsilon_2\left(\frac{\omega}{1+\lambda}\right) \tag{3}$$

and in Ref. 18 the optical conductivity is

$$\hat{\sigma}(\omega) = \frac{1}{(1+\lambda)^2}\sigma\left(\frac{\omega}{1+\lambda}\right). \tag{4}$$

Both formulas do not satisfy the sum rule

$$\int_0^\infty \sigma(\omega)d\omega = \frac{\pi n e^2}{2m}, \tag{5}$$

where m, e, and n are the electronic mass, charge, and concentration, respectively. In Ref. 19 the λ-fitted optical conductivity is given by

$$\hat{\sigma}(\omega) = \frac{1}{1+\lambda}\sigma\left(\frac{\omega}{1+\lambda}\right), \tag{6}$$

which satisfies the sum rule of Eq. (5). Therefore the denominator of the prefactor of right hand side of Eq. (3) should be squared and that of Eq. (4) should not be squared. Both experimental and theoretical (with and without the λ fitting) spectra are shown in Fig. 4. The broadened optical-conductivity spectrum reproduces the shape of the experimental one, however, the magnitude and peak position do not match. With $\lambda = -0.18$ the shape and the magnitude of the theoretical spectra agree fairly well with the experimental one. The absolute value of λ is larger than those of CoAl ($\lambda = -0.15$) (Ref. 19) and Ni ($\lambda = -0.12$).[18]

Before broadening and λ fitting we did not include any adjustable or empirical parameters to make the theoretical spectrum coincide with the measured one. The broadening and λ fitting are optimized to give a theoretical spectrum which agrees with the measured one in both the magnitude and the energy position of the 4.4 eV peak.

We have identified the band pair and tetrahedra (regions in $\mathbf{k}$ space) which provide the dominant contributions to the various spectral features by keeping track of that information during the optical-conductivity calculations with appropriate energy windows (defining the different spectral features). The main contribution to the 4.4 eV peak (5.5 eV peak in the theory) arises from transitions initiating from band 3 (50% of Ni d character and 50% of mixture of Ni and Al sp character) to $\mathbf{k}$ points of the Γ-M-R plane and the midpoints of the near X-M line and the Γ-M line to band 18 (having a similar character to band 3). The strong transitions are shown by long arrows in Fig. 2. Very small contributions come from the transitions from band 2 to band 16 located just above E_F at the $\mathbf{k}$ point near the Γ point. Overall there are only small contributions from $\mathbf{k}$ points in the neighborhood of the Γ point, unlike the conclusion of Ref. 12.

With the inclusion of the dipole-transition-matrix elements we found large peaks around the 5.5 eV region, while there are two peaks at 3.4 and 3.9 eV in Ref. 12 where the dipole-transition-matrix elements are not included. Although the dipole-transition-matrix elements were included in the calculation of the optical-conductivity in Ref. 10, the authors assign the two peaks in their calculated optical conductivity spectrum to the same origin of $\mathbf{k}$ points as that of Ref. 12. The two peaks are not explicitly identified in Ref. 10, however, we assume that they are the ones shown at 4.8 and 5.5 eV. The assignments are not correct for two reasons; first, the inclusion of the dipole-transition-matrix elements in the optical-conductivity calculation changes the peak positions in the optical spectra from the assignments of Ref. 12, and second, the energies of the two transitions listed do not agree with the peak positions of the calculated spectrum, e.g., we find ~3.8 eV for the transitions from bands 3 and 4 to bands 14 and 15 near the Γ point and ~3.23 eV for the transitions from bands 5 and 6 to bands 14 and 15 near the same symmetry point.

In Ref. 12 there is a weak shoulder around 0.8 eV in the experimental spectrum. After broadening and λ fitting our calculation shows a strong peak at 1 eV and we assign this peak to the shoulder around 0.8 eV. For this peak most of the strong transitions arise from $\mathbf{k}$ points near the M point, from band 9 (mainly Ni d character) to bands 18 and 19 (50% of Ni d character and 50% of mixture of Ni and Al sp character), and 1/3 way of Γ-X line, from band 17 (mainly Ni d character) to band 18.

In summary, we have measured the dielectric functions of Ni_3Al alloys. Our measured optical conductivity is almost 50% larger than a previous measurement.[12] The discrepancy was hypothesized to be due to the rough overlayer of the previous sample. The rough overlayer was modeled as a mixture of void and bulk and the fitting results provide a plausible explanation for the difference in the two measurements. Band structure and optical-conductivity spectra were

calculated using the LAPW method. The calculated optical conductivity, with empirically adjusted real (λ fitting) and imaginary (broadening) parts of the quasiparticle self-energy, exhibits good agreement with experiment. The origin of the main peak (4.4 eV) of the optical-conductivity spectrum is transitions at the **k** points near the Γ-M-R plane and midpoints of the X-M line and the Γ-M line from band 3 to band 18; both bands are similar, with at least 50% Ni d characters, with the dipole transitions primarily from p-d matrix elements on the Ni site.

We wish to thank Professor K. A. Gschneidner, Jr. for providing Ni_3Al alloys. The Ames Laboratory is operated for the U. S. Department of Energy by Iowa State University under Contract No. W-7405-Eng-82.

[1] Y. Noda, S. M. Shapiro, G. Shirane, Y. Yamada, and L. E. Tanner, Phys. Rev. B **42**, 10 397 (1990), and references therein.
[2] F. R. de Boer, C. J. Schinkel, J. Biesterbos, and S. Proost, J. Appl. Phys. **40**, 1049 (1969).
[3] S. K. Dhar and K. A. Gschneidner, Jr., Phys. Rev. B **39**, 7453 (1989).
[4] S. K. Dhar, K. A. Gschneidner, Jr., L. L. Miller, and D. C. Johnston, Phys. Rev. B **40**, 11 488 (1989).
[5] D. Hackenbracht and J. Kübler, J. Phys. F **10**, 427 (1980).
[6] J. J. M. Buiting, J. Kübler, and F. M. Mueller, J. Phys. F **13**, L179 (1983).
[7] B. I. Min, A. J. Freeman, and H. J. F. Jansen, Phys. Rev. B **37**, 6757 (1988).
[8] J. Xu, B. I. Min, A. J. Freeman, and T. Oguchi, Phys. Rev. B **41**, 5010 (1990).
[9] M. A. Khan, A. Kashyap, A. K. Solanki, T. Nautiyal, and S. Auluck, Phys. Rev. B **48**, 16 974 (1993).
[10] F. R. de Boer, J. J. M. Franse, and P. E. Brommer, Physica B+C **106B**, 1 (1981).
[11] P. A. M. van der Heide, J. J. M. Buiting, L. M. ten Dam, L. W. M. Schreurs, R. A. de Groot, and A. R. de Vroomen, J. Phys. F **15**, 1195 (1985).
[12] J. F. Janak, A. R. Williams, and V. L. Moruzzi, Phys. Rev. B **11**, 1522 (1975).
[13] J. Y. Rhee, Ph.D. thesis, Iowa State University, 1992 (unpublished), and references therein.
[14] D. A. G. Bruggeman, Ann. Phys. (Leipzig) **24**, 636 (1935).
[15] D. E. Aspnes, E. Kinsbron, and D. D. Bacon, Phys. Rev. B **21**, 3291 (1980).
[16] D. D. Koelling and B. N. Harmon, J. Phys. C **10**, 3170 (1977).
[17] L. Hedin and B. I. Lundqvist, J. Phys. C **4**, 2064 (1971).
[18] D. G. Laurent, J. Callaway, and C. S. Wang, Phys. Rev. B **20**, 1134 (1979).
[19] K. J. Kim, B. N. Harmon, and D. W. Lynch, Phys. Rev. B **43**, 1948 (1991).